International Journal of Nanomedicine

Dovepress
Taylor & Francis Group

Open Access Full Text Article

ORIGINAL RESEARCH

Graphene Oxide Nanosheets Induce Mitochondrial Toxicity in Human Ovarian Granulosa Cells: Implications for Female Reproductive Health

Min Li*, Hedong Lu*, Chunya Ye*, Xiaolei Wang, Dongmei Ji, Zhiguo Zhang, Yunxia Cao, Weiwei Zou

Department of Obstetrics and Gynecology, The First Affiliated Hospital of Anhui Medical University, Hefei, 230022, People's Republic of China

*These authors contributed equally to this work

Correspondence: Yunxia Cao; Weiwei Zou, Department of Obstetrics and Gynecology, The First Affiliated Hospital of Anhui Medical University, No. 218 Jixi Road, Hefei, 230022, People's Republic of China, Email caoyunxia@ahmu.edu.cn; tottizou@126.com

Purpose: Graphene oxide (GO) has promising biomedical applications, but its potential toxicity to the female reproductive system is underexplored. This study investigates the short-term effects of a single dose of GO nanosheets on human ovarian granulosa cells, focusing on mitochondrial damage.

Materials and Methods: First, cell viability was detected by CCK-8 and apoptosis was detected by flow cytometry to assess the cytotoxicity of GO on KGN. Second, reactive oxygen species (ROS), mitochondrial membrane potential (MMP), and mitochondrial morphology were observed by confocal microscopy, mitochondrial and sub-mitochondrial structure by transmission electron microscopy (TEM), quantitative analysis of ATP and mitochondrial complex I enzyme activity by luminosity value and autophagy by flow cytometry to assess the mitochondrial toxicity of GO on KGN cells.

Results: The 72h half-maximum effective concentration (EC50) value of GO was determined to be 29.73 μg/mL. GO induced cell death in a dose-dependent manner, with significant effects on cell viability even at low doses (1 μg/mL). Exposure to low GO concentrations resulted in abnormal mitochondrial morphology and function, including mitochondrial breakage, membrane damage, reduced mitochondrial cristae, enhanced autophagy, decreased ATP production, decreased MMP, and decreased enzymatic activity of mitochondrial complex I. Mitochondrial function returned to normal levels on day 7 after KGN cells left the GO-exposed environment.

Conclusion: This study demonstrates that short-term exposure to low-dose GO causes mitochondrial damage in human ovarian granulosa cells, highlighting the need for further research on the safety of GO, particularly regarding its potential effects on reproductive health. However, GO-induced transient mitochondrial damage is highly likely to negatively affect ovarian reserve function, which needs to be further verified in animal models.

Keywords: graphene oxide, human ovarian granulosa cells, mitochondrial damage, cytotoxicity, reproductive toxicity

Introduction

Two-dimensional (2D) nanomaterials began with the successful advent of single-layer graphene in 2004 and have developed rapidly.[1] Due to its excellent electronic and thermal conductivity, as well as mechanical properties, graphene is increasingly used in biomedical applications.[2] Graphene Oxide (GO) is a derivative of graphene, and its superior colloidal properties and dispersibility make the material extremely attractive in biomedical applications, including antimicrobials, biosensing, bioimaging, and drug delivery.[3–8] Due to its high stability and biocompatibility, GO also has applications in the field of reproductive medicine, such as improving in vitro fertilization.[9,10]

Received: 17 October 2024
Accepted: 25 March 2025
Published: 10 April 2025

© 2025 Li et al. This work is published and licensed by Dove Medical Press Limited. The full terms of this license are available at https://www.dovepress.com/terms.php and incorporate the Creative Commons Attribution – Non Commercial (unported, v4.0) License (http://creativecommons.org/licenses/by-nc/4.0/). By accessing the work you hereby accept the Terms. Non-commercial uses of the work are permitted without any further permission from Dove Medical Press Limited, provided the work is properly attributed. For permission for commercial use of this work, please see paragraphs 4.2 and 5 of our Terms (https://www.dovepress.com/terms.php).

Graphical Abstract

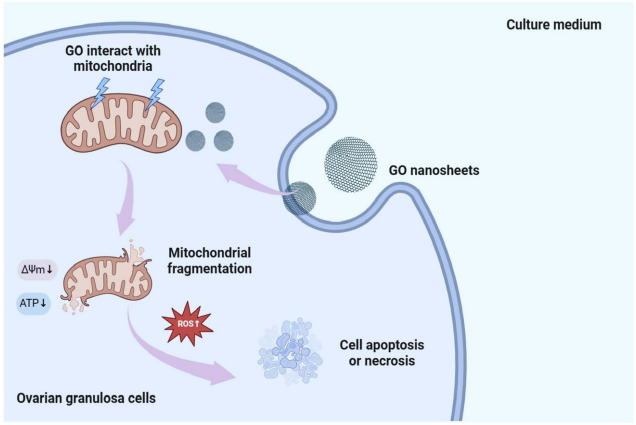

However, the risk of exposure to GO has increased due to the increasing potential applications of GO in the biomedical field. According to previous studies, GO exposure occurs via several routes, including intravenous injection, subcutaneous injection, intraperitoneal injection, oral gavage, and intratracheal instillation.[11–15] In addition, GO can also accumulate in tissues and organs through biological barriers such as blood tests and blood-placental barriers, and cause acute and chronic toxicity.[16,17] Therefore, its potential toxicity remains a significant concern, especially in the context of human reproductive health. Graphene oxide has been shown to enter cells via endocytosis or phagocytosis and induce cytotoxicity such as oxidative stress and mitochondrial dysfunction in a dose-dependent manner in a variety of cell types.[18,19] However, its effects on the female reproductive system are not well understood, whether short-term effects (germ apoptosis) or long-term effects (impaired fertility).

Mitochondria are key organelles with a bilayer membrane structure, which can be divided into the outer mitochondrial membrane (OMM), mitochondrial membrane space, inner mitochondrial membrane (IMM), and mitochondrial matrix from the outside to the inside.[20] The IMM folds towards the mitochondrial matrix to form mitochondrial cristae. They undergo a continuous and stable process of division and fusion through the membrane, forming a dynamic interconnected network to preserve the integrity of the mitochondrial functional network.[21,22] Given that the ATP synthase complex and the mitochondrial electron transport chain (ETC) are located in the mitochondrial cristae, the integrity of cristae morphology is critical for mitochondrial function. Mitochondria are involved in regulating signal transduction, electron transport, aerobic phosphorylation, calcium homeostasis, and other cellular functions, and are therefore critical in maintaining intracellular homeostasis.[23,24] In addition, mitochondria are the main sites for energy conversion to produce most of the energy that cells use to sustain life, as well as to produce ROS.[25] Normally, intracellular ROS is beneficial for regulating cellular function. However, excessive ROS accumulation caused by mitochondrial dysfunction can further lead to oxidative stress, decreased mitochondrial membrane potential (MMP), and impaired mitochondrial structure. Mitophagy is activated when mitochondrial damage occurs due to oxidative stress in cells. Autophagy selectively removes abnormal mitochondria to maintain mitochondrial homeostasis and prevent cells from being further damaged.[26,27]

Previous studies have shown that the ovaries exhibit a high degree of sensitivity to the invasion of foreign particles and chemicals and lead to reproductive toxicity such as premature ovarian failure, follicular atresia, hormonal imbalances, delayed puberty, and increased incidence of female infertility.[28,29] Ovarian granulosa cells, which are crucial for hormone synthesis and oocyte maturation, play a vital role in female fertility.[30,31] Ovarian granulosa cells are also involved in the synthesis of important growth factors required during oocyte development to maintain the microenvironment required for oocyte growth and maturation.[31] Damage to ovarian granulosa cells can disrupt the normal

reproductive process and lead to hormonal imbalances, follicular atresia, and impaired oocyte growth and development.[32] Studies have shown that mitochondrial dysfunction in human granulosa cells may lead to decreased steroid production, fertilization rates, oocyte maturation rates, and oocyte quality, ultimately endangering fertility.[33] Previous studies on the toxicity of GO have shown that GO internalization can disrupt mitochondrial homeostasis by activating NOX2 signaling to increase ROS in neuroblastoma cells, but its effects on ovarian granulosa cells are unclear.[34] This study aims to fill this gap by evaluating the effects of GO nanosheets on mitochondrial function and cell viability in human ovarian granulosa cells, providing crucial insight into the potential risks of GO exposure on female reproductive health.

Materials and Methods

Materials

Dulbecco's modified Eagle's medium (DMEM), fetal bovine serum (FBS), and penicillin-streptomycin were purchased from Gibco (Thermo Fisher Scientific, Waltham, USA). Mito-Tracker Deep Red FM (MTDR) was obtained from Invitrogen (Thermo Fisher Scientific, Waltham, USA). The detection dye for autophagy (DAPGreen) was purchased from Dojindo Molecular Technologies, Inc. (Japan) and Graphene oxide nanosheets were gifts from the laboratory of Professor Qixin Chen of Shandong First Medical University.

Cell Line Culture

The ovarian granulosa cell line KGN has been widely used as an in vitro model for various studies related to female reproductive function.[35,36] The human ovarian granulosa cell line KGN was a gift from Associate Professor Yajing Liu of Anhui Medical University. The cell line KGN was cultured in DMEM supplemented with 10% FBS and 1% penicillin-streptomycin antibiotic. The cells were cultured in a cell culture incubator (Thermo Fisher Scientific, Waltham, USA) at 37°C, 100% humidity, and 5% CO_2.

Preparation of GO Nanosheet Solutions and Characterization of GO

According to the previous protocol,[37] before cell experiments, GO nanosheet dispersion solution was first prepared in PBS at a concentration of 10 μg/mL by sonication. Dilute to different treatment concentrations with DMEM solution with 10% FBS and disperse by sonication (50 W, 30 min). The topography of GO nanosheets was assessed using atomic force microscopy (AFM, NanoWizard 4XP, Bruck, Massachusetts, USA).

CCK-8 Cytotoxicity Assay

Cytotoxicity of cells treated with GO nanosheets at different concentrations was detected by a Cell Counting Kit-8 (CCK-8, Beyotime, Shanghai, China). The cells were seeded in 96-well plates with 5×10^3 cells/well. After adherent incubation for 24 h, the KGN cells were treated with GO nanosheets at increasing concentrations (0.1, 1, 10, 50, and 100 μg/mL) for 48 h and 72 h. The control group was treated with the complete medium. After 48–72h of GO nanosheet treatment, cells were washed three times with phosphate buffered saline (PBS). 100 μL of 10% CCK-8 solution was added to each well, and incubated in a 37°C incubator for one hour, and the absorbance at 450 nm was detected using a multifunctional microplate reader (Molecular Devices, Sunnyvale, USA). Cell viability was calculated as per the previous protocol.[38] In this experiment, six replicates were set up for each concentration, and three biological replicates were performed.

Flow Cytometry Analysis of Apoptosis

Apoptosis was determined using the FITC-Annexin V/PI Apoptosis Assay Kit (UElandy, Suzhou, China). The experimental group cultured KGN cells with a final concentration of 1 μg/mL GO nanosheet solution for 72 h, and the control group was supplemented with an equal volume of fresh complete medium. After 72 h, KGN cells were collected by centrifugation at 1000 rpm for 5 min following the manufacturer's instructions and washed twice with PBS. The KGN cells were resuspended with PBS and cell density was calculated, and 1×10^5 cells were centrifuged at 1000 rpm for 5 min. Resuspended the cells in 100 μL of 1× Annexin V binding buffer and added 5 μL Annexin V-fluorescein

isothiocyanate (FITC) and 5 μL PI working solution. The KGN cells were incubated at room temperature (20–25°C) for 15 min in the dark. After the incubation was complete, 400 μL of 1× Annexin V binding buffer was added and gently mixed. Before testing, all samples were kept on ice, and testing of all samples was required to be completed within one hour. Apoptosis assay was performed essentially as previously described.[38] Data were collected using a FACS Calibur flow cytometer (BD Biosciences, Franklin Lakes, USA) and analyzed using FlowJo software to quantify apoptotic cells. The experiment was independently assayed three times.

Quantitative Analysis of Cellular Reactive Oxygen Species (ROS)

The effect of GO nanosheets on ROS production in human ovarian granule cell line KGN was analyzed using the DCFDA/H2DCFDA-Cellular ROS Assay Kit (Abcam, Waltham, USA). The KGN cells were cultured on six-well culture plates. The cells were then treated with 1 μg/mL GO nanosheets and incubated at 37°C in a 5% CO_2 incubator for 72 h. The control group was treated with fresh complete medium without GO nanosheets. After 72 h of treatment, the cells were rinsed twice with buffer. 20 μM DCFHDA was added to each group and incubated in a 37°C incubator for 45 minutes in the dark. After 45 min, the cells of each group were washed three times with buffer and resuspended in buffer protected from light. Cells were then added to a black-edged, clear-bottomed 96-well plate (2.5×10^4 cells/well) and immediately measured at Ex/Em=485/535 nm in endpoint mode on a fluorescence plate reader (Molecular Devices, Sunnyvale, USA) to quantify ROS.[39] The experiment was independently tested three times.

ATP Content Assay

The KGN cells were cultured on six-well plates, then treated with 1 μg/mL GO nanosheets and incubated for 72 h at 37°C in a 5% CO_2 incubator. The cells were treated according to the instructions of the manufacturer of the ATP Bioluminescence Detection Kit CLS II (Roche, Basel, Switzerland). The KGN cells were collected by centrifugation at 1000 rpm for 5 min and washed twice with PBS. The KGN cells were resuspended with PBS and cell density was calculated, and 2×10^5 cells were centrifuged at 1000 rpm for 5 min. The KGN cells were resuspended in 150 μL of distilled water and 150 μL of lysate, and KGN cells were incubated for 10 minutes at room temperature (20–25°C). After incubation, the cells were centrifuged at 12,000 rpm for 1 min, and then the supernatant was transferred to a new 1.5 mL centrifuge tube and kept on ice. ATP standards were gradually diluted with distilled water to 10^{-10}–10^{-5} M. Transfer the treated cell supernatant and ATP standard to a white-walled opaque bottom 96-well plate (Beyotime, Shanghai, China). Read the luminescence by a multimode microplate reader (Molecular Devices, Sunnyvale, USA). The assay was independently tested three times.

Confocal Fluorescence Imaging of MMP

MMP fluorescence analysis based on previous protocols.[40,41] The KGN cells were treated with 1 μg/mL of GO nanosheets for 72 h. GO nanosheet-treated and untreated cells were subcultured in glass-bottom dishes and incubated for 24 h. The KGN cells were washed twice with PBS and stained with Rhodamine 123 at a concentration of 10 μg/mL and incubated in a 37°C incubator for 20 min in the dark. Hoechst-33342 (Beyotime, Shanghai, China) dye is used for staining nuclei. Cells were washed twice with PBS and then stained with Hoechst 33342 dye (10 μg/mL) and incubated for 20 min at 37°C away from light. After the end of the incubation, the cells were washed three times with PBS and observed under a confocal laser scanning microscope. All images were acquired by ZEISS LSM-980 confocal laser scanning microscope (Carl Zeiss, Inc., Jena, Germany) and analyzed using ZEN version 3.8 software (Carl Zeiss, Inc., Jena, Germany) and ImageJ software (https://imagej.nih.gov/ij/).

Mitochondrial Permeability Transition Pore (mPTP) Analysis

MPTP analysis was performed according to the protocol of the previous study.[34] MPTP was studied using the mPTP assay kit (Beyotime, Shanghai, China). KGN cells were treated with 1 μg/mL GO nanosheets and cultured in a 37°C incubator with 5% CO_2 for 72 h. Then, GO nanosheet-treated and untreated cells were subcultured in glass-bottom petri dishes for 24 h. KGN cells were stained with 0.5× calcein AM, 1× fluorescent quenching agent $CoCl_2$, or 1 μM positive treatment Ionomycin and incubated for 45 min at 37°C in the dark. After incubation, replaced with fresh complete

medium and incubated for 30 min at 37°C in the dark. After staining, the cells were washed once with PBS and then twice with DMEM to thoroughly remove residual reagents and observed under a fluorescence microscope. All images were acquired by ZEISS LSM-980 confocal laser scanning microscope (Carl Zeiss, Inc., Jena, Germany).

Mitochondrial Complex I Activity Assay

Mitochondrial complex I activity was assayed using the complex I enzyme activity assay kit (Abcam, Waltham, USA). KGN cells were treated with 1 μg/mL GO nanosheets and cultured in a 37°C incubator with 5% CO_2 for 72 h. Mitochondrial complex I activity assay was performed according to the previous protocol.[42] Briefly, KGN cells were resuspended with DMEM and washed twice with PBS. 1×10^7 cells were collected by centrifugation at 1000 rpm for 5 min. Proteins were then extracted with 1/10 of the cell suspension, and protein concentrations were subsequently measured using a BCA protein assay kit (Thermo Fisher Scientific, Waltham, USA). Adjust the remaining cells to achieve a final protein concentration of 5.5 mg/mL. Detergent equivalent to one-tenth of the pellet volume was added and the mixture was incubated for 30 min (maintained on ice). Centrifugation at 16,000 rpm for 20 min at 4°C, collected the supernatant, and diluted the protein to 1000 μg/mL with the incubation solution. After incubation, wash buffer (300 μL, 1×) was added to each well and washed three times. Finally, added 200 μL of working solution to each well in the dark. The absorbance at 450 nm was detected using a multifunctional microplate reader (Molecular Devices, Sunnyvale, USA).

Confocal Fluorescence Imaging and Quantification of Mitochondrial Morphology

The KGN cells were cultured on six-well plates, then treated with 1 μg/mL GO nanosheets and incubated for 72 h at 37°C in a 5% CO_2 incubator. GO nanosheet-treated and untreated cells were subcultured in glass-bottom dishes (BS-20-GJM, Biosharp, Hefei, China) and incubated for 24 h. The KGN cells were washed twice with PBS and stained with 100 nM MTDR (Thermo Fisher Scientific, Waltham, USA) and incubated in a 37°C incubator for 30 min in the dark. After the end of the incubation, the cells were washed three times with DMEM and observed under a confocal microscope. All images were acquired by ZEISS LSM-980 confocal laser scanning microscope (Carl Zeiss, Inc., Jena, Germany).

Mitochondrial morphology quantification was performed as previously described.[43] Briefly, fluorescence images of a single cell containing bright mitochondria are imported into the ImageJ software (https://imagej.nih.gov/ij/). First, change the image type and adjust the threshold. Check the area, shape descriptor, and threshold limit in the "Set Measurements" option, and then click "Analyze Particles" to get the "L/W" ratio (data in the "AR" column).

Transmission Electron Microscopy (TEM)

Mitochondrial and submitochondrial structures were observed using electron microscopy. The KGN cells were cultured on six-well plates, then treated with 1 μg/mL GO nanosheets and incubated for 72 h at 37°C in a 5% CO_2 incubator. Cells were collected by centrifugation at 1000 rpm for 5 min. TEM photography was performed as per the previous protocol.[37] GO nanosheet-treated and untreated cell samples were dehydrated after fixation and embedded in Alalite. Subsequently, ultrathin sections were placed on a coated grid. Individual sections were stained and observed under a TEM (Tecnai T12, FEI, Inc, Hillsboro, USA) at an accelerating voltage of 120 kV.

Autophagy

Autophagy was detected by the autophagosome detection probe DAPGreen (Dojindo Molecular Technologies, Inc., Kumamoto, Japan). KGN cells were incubated in a 37°C incubator for 72 h with and without GO nanosheets. After treatment, the cells were washed twice with PBS and incubated with DAPGreen dye (0.1 μM) for 30 min at 37°C following the manufacturer's instructions. Finally, data were collected using a FACS Calibur flow cytometer (BD Biosciences, Franklin Lakes, USA) and quantified using FlowJo software. The assay was independently tested three times.

Data Statistics and Analysis

The different types of experiments were repeated independently more than three times, and each treatment of each independent experiment was assessed more than twice. The results were similar, and all images shown were

representative results of biological replicates. Statistical differences between GO-treated and untreated groups were determined using Student's *t*-test. The statistical significance of differences in means was determined using Tukey's post hoc test (for comparisons between multiple groups). Statistical differences were analyzed and all results were plotted via GraphPad Prism 9.4.1 (GraphPad Software Inc., California, USA). All experimental values are expressed as Mean ± SEM (standard error of the mean), with p-values < 0.05 being recognized as statistically significant. *$p < 0.05$; **$p < 0.01$; ***$p < 0.001$; ****$p < 0.0001$. EC50 value was calculated using the nonlinear regression model "log[agonist] vs response-variable slope (four parameters)" in GraphPad Prism 9.4.1 software.

Results

Cytotoxicity of GO Nanosheets

Studies have found that physical chemistry such as the size and functional groups of GO nanomaterials can greatly affect their biological behavior, resulting in a wide variety of effects on cell viability and function.[44,45] In view of this, we characterized GO nanosheets by atomic force microscopy (AFM) before studying their cytotoxicity to KGN cells. The results show that the lateral size of GO nanosheets can reach 3 μm and the thickness can reach tens of nanometers (Figure S1). The single GO nanosheets used in this study were obtained from Graphene Supermarket (NY, USA). Graphene oxide can be dissolved in water because its oxygen-containing groups have a high affinity to water molecules.[2] The GO nanosheets used in this study have good dispersion in aqueous solutions.

As the largest population of cells in the follicle, ovarian granulosa cells play a key role in ovarian functional activities such as follicular growth and development and estrogen production and are also involved in maintaining the microenvironment required for oocyte growth and maturation. Apoptosis of ovarian granulosa cells will inevitably lead to abnormal follicular development and sex hormone levels. Therefore, we chose the ovarian granulosa cell line KGN as a cell model to study the potential damage of GO nanosheets to the female reproductive system in vitro.

To understand whether GO causes cytotoxicity in human ovarian granulosa cells, we first incubated different concentrations (0.1, 1, 10, 50, and 100 μg/mL) of GO nanosheets with KGN cells for 48 h and 72 h, respectively. We then used CCK-8 to determine the effect of GO on the cell viability of KGN. We measured the cell viability of KGN cells treated with GO nanosheets at different concentrations. As shown in Figure 1A, a tendency to decrease in cell viability in a time- and dose-dependent manner was observed at different periods of 48 h and 72 h when the KGN cells were treated with GO nanosheets. We found that the cell viability was approximately 65% when cells were exposed to 100 μg/mL GO nanosheets for 48 h, and further decreased to 45% when the incubation time was increased to 72 h. Cell viability was approximately 70% when cells were exposed to 50 μg/mL GO nanosheets for 48 h and further decreased to 52% when the incubation time was increased to 72 h. When exposed to GO nanosheets for 72 hours, KGN cells maintained high cell viability at concentrations up to 10 μg/mL, with a viable cell rate of nearly 80%. However, when cells were exposed to GO nanosheets for 48 h, the cell viability of KGN cells was significantly affected even at low concentrations (0.1 and 1 μg/mL) of GO nanosheets compared to normal cells. In addition, the 72h half-maximum effective concentration (72h-EC50) value of GO nanosheets was determined to be 29.73 μg/mL using a regression model (Figure S2). A previous study observing the reproductive toxicity of GO in Japanese medaka showed that the germ cell development of females only began to show abnormalities at doses higher than 1 μg/mL.[46] This suggests that 1 μg/mL may be the lowest threshold for reproductive toxicity caused by GO. Therefore, we chose 1 μg/mL as the treatment dose of GO in our experiments to observe the damage caused by very low doses of GO on mitochondria of human ovarian granulosa cells.

To further explore the potential patterns or types of KGN cell death induced by GO nanosheets, we employed FITC-Annexin V/PI to detect apoptosis. As shown in Figure 1B, exposure to GO nanosheets at a concentration of 1 μg/mL resulted in 14.2% apoptosis and 7.99% necrosis. Treatment with GO nanosheets resulted in a significant increase in the overall apoptosis rate in cells compared to the control group (Figure 1C). In summary, our findings suggested that despite the promising biocompatibility of some GO-based applications and biologics,[47,48] GO still exhibits inevitable cytotoxicity, including the induction of apoptosis. This underscores the importance of carefully determining the safe dosage range for all GO-based biomedical applications.

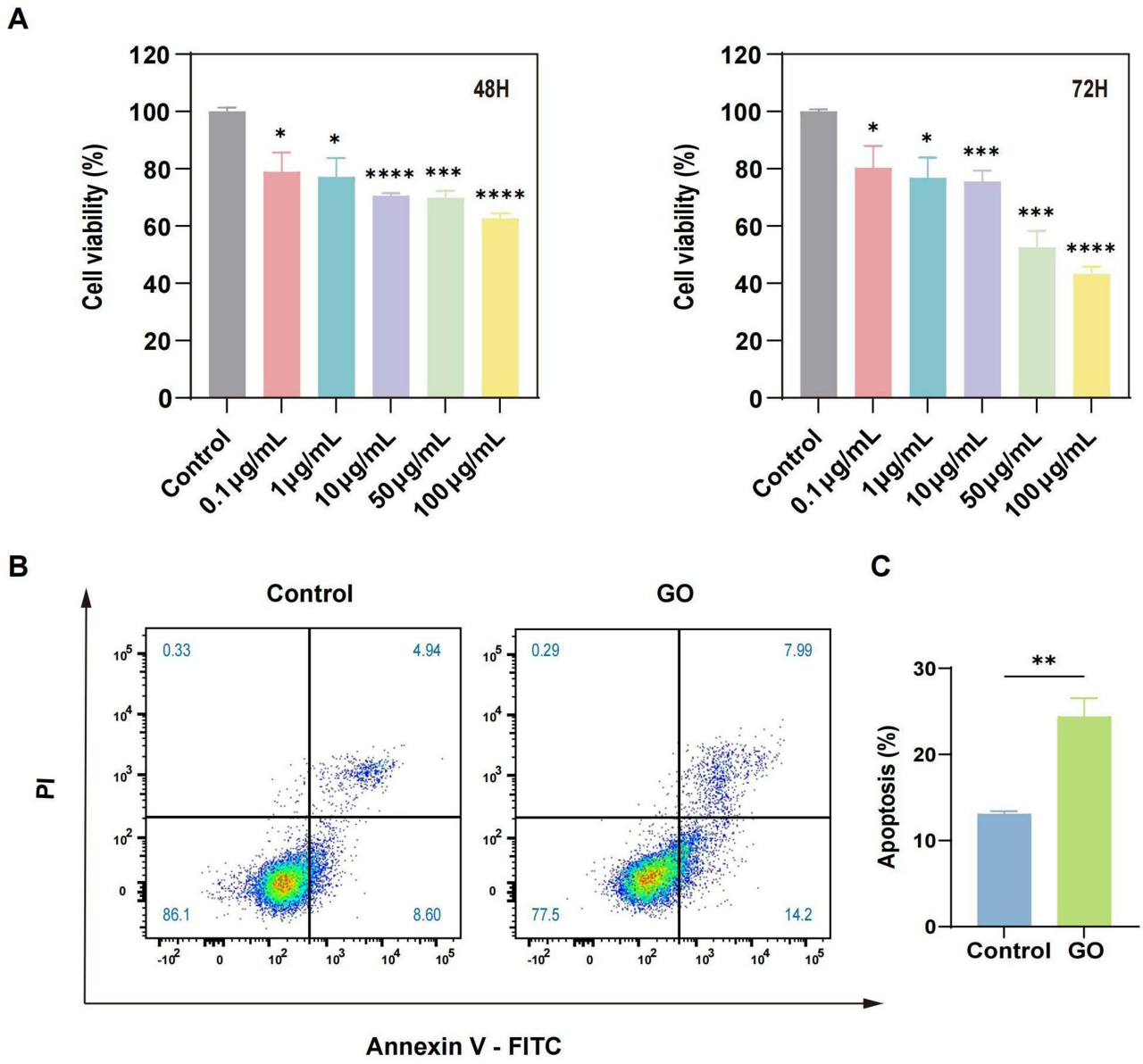

Figure 1 Cytotoxic effects of graphene oxide nanosheets on KGN cells. (**A**) Human ovarian granulosa cells were cultured and exposed to graphene oxide nanosheets (0.1–100 μg/mL) at varying concentrations for 48 h and 72 h, respectively. Subsequently, a CCK-8 assay was conducted to determine the percentage of viable cells that were expressed. (**B**) Flow cytometry was used to analyze apoptosis in KGN cells treated with Annexin V-FITC/PI after 72 h of different treatments. (**C**) Quantitative analysis of the ratio of apoptosis and cell necrosis in (**B**). Data are expressed as Mean ± SEM (n=3). Statistical differences between experimental groups were analyzed by the Student's *t*-test. **p* < 0.05, ***p* < 0.01, ****p* < 0.001 and *****p* < 0.0001.

GO Nanosheets Interact With Mitochondria After Being Engulfed by Cells

Studies have shown that the sharp edges of nanomaterials can interact with cell membranes.[49] Therefore, we hypothesize that GO nanosheets can enter cells and cause a series of cellular changes that ultimately lead to cell death. To verify this hypothesis, we further investigated the deposition and distribution of GO nanosheets in cells. Transmission electron microscopy (TEM) was used to observe that GO nanosheets could be engulfed by cells and deposited intracellularly (Figure 2A). Mitochondria often play a key role in cell apoptosis.[50] To determine whether GO nanosheets affect mitochondria, we investigated the effect of GO nanosheets on mitochondrial structure by performing TEM imaging on normal cells and GO nanosheet-treated cells. The results showed that GO nanosheet treatment disrupted the integrity of the mitochondrial cristae compared to healthy mitochondria with clear cristae structure observed in normal cells (Figure 2B), preliminarily suggesting that GO nanosheets can indeed be engulfed by cells and that GO can interact

https://doi.org/10.2147/IJN.S495259

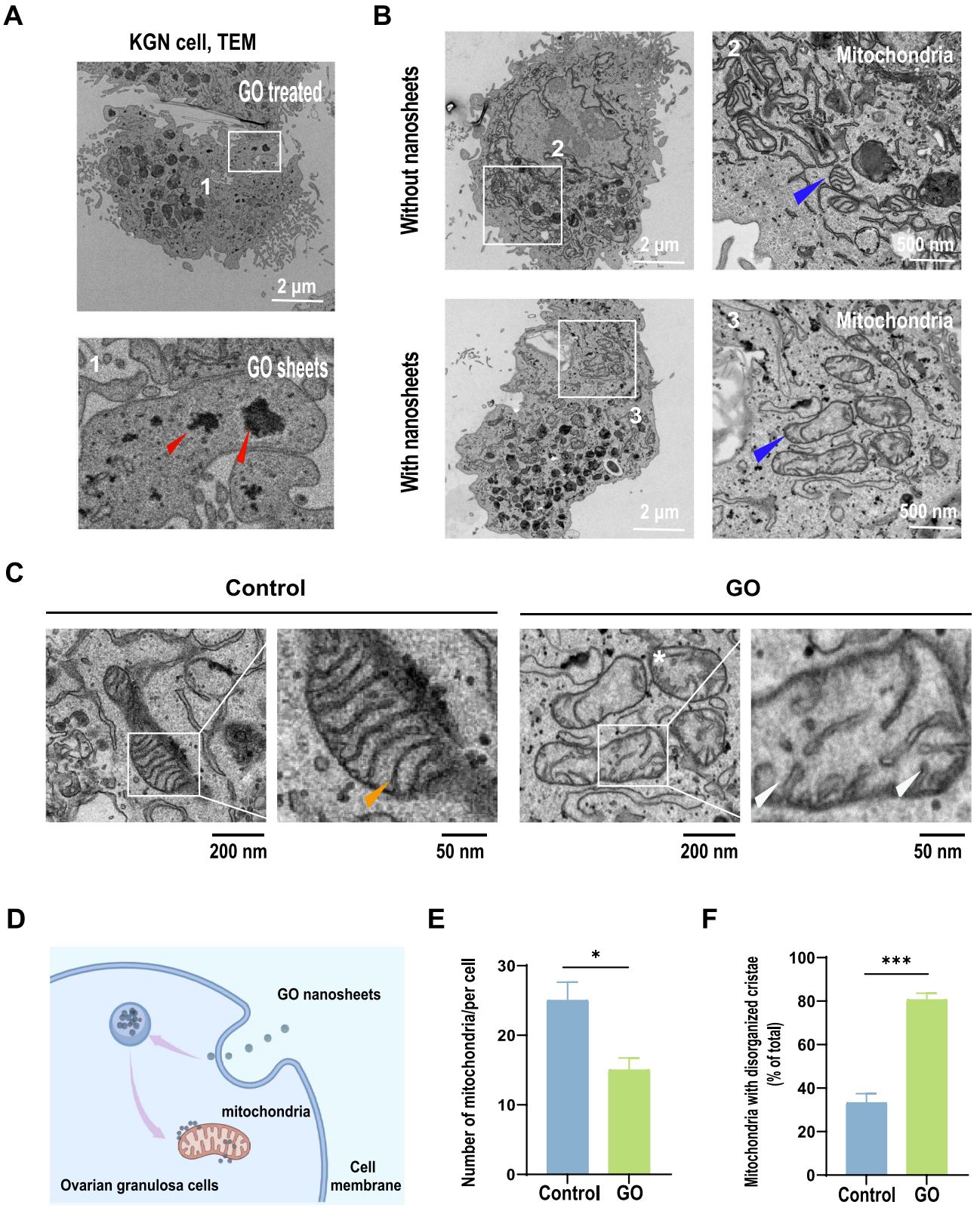

Figure 2 GO nanosheets enter the living cells and interact with mitochondria. (**A**) TEM image of KGN cells co-incubated with 1 μg/mL GO and distribution of GO in living cells. (**B**) Representative TEM images and magnified regions of interest of GO nanosheet-treated and untreated KGN cells. The image showed that GO entered the cell and interacted with the mitochondria, resulting in mitochondrial damage. (**C**) TEM images of mitochondria at higher magnification, with the control group showing well-defined mitochondrial cristae (Orange arrow) and normal inner mitochondrial membrane (IMM) invagination. The GO nanosheet treatment group showed a decrease in the number of cristae (white arrows), abnormal invagination and dissolution of the IMM (*). (**D**) Schematic diagram of GO's distribution in KGN cells. Quantitative analysis of the number of mitochondria. (**E**) and the proportion of damaged mitochondria. (**F**) in normal cells and graphene oxide-treated cells. Statistical differences between experimental groups were analyzed by the Student's *t*-test, and results were expressed as Mean ± SEM (n=3). *$p < 0.05$, ***$p < 0.001$.

with mitochondria once it enters the cell, leading to mitochondrial damage. To further observe mitochondrial and submitochondrial structures, representative transmission electron microscopy (TEM) images of mitochondria from both groups of cells were performed at higher magnification (Figure 2C). The mitochondria of the cells in the control group showed clearly visible mitochondrial cristae, which are complemented by a densely packed mitochondrial matrix. The inner mitochondrial membrane (IMM) of the control group was normally invaginated. In contrast, mitochondria in the GO nanosheet-treated group exhibited abnormal invagination and dissolution of IMM. In addition, the GO nanosheet treatment group exhibited a reduced number and structural disorder of mitochondrial cristae and brighter mitochondrial matrix. Damage to mitochondrial membrane structure and submitochondrial structure may be caused by the interaction between GO nanosheets and mitochondria after being engulfed by cells and deposited around the mitochondria (Figure 2D). We also observed a decrease in the number of mitochondria (Figure 2E). Subsequently, we quantified healthy mitochondria and damaged mitochondria from normal cells and GO nanosheet-treated cells. As shown in Figure 2F, GO nanosheet treatment resulted in significant mitochondrial damage compared to control cells, with the proportion of abnormal mitochondria being as high as 80% and healthy mitochondria being only 20%. In summary, GO nanosheets can indeed induce apoptosis by damaging mitochondria, which is consistent with previous reports.[50]

GO Nanosheet Treatment Induces Autophagy

To survive, cells may trigger autophagy to eliminate damaged mitochondria. Through TEM imaging, we observed an increase in autophagosomes in GO nanosheet-treated cells compared to normal cells (Figure 3A and B). To investigate

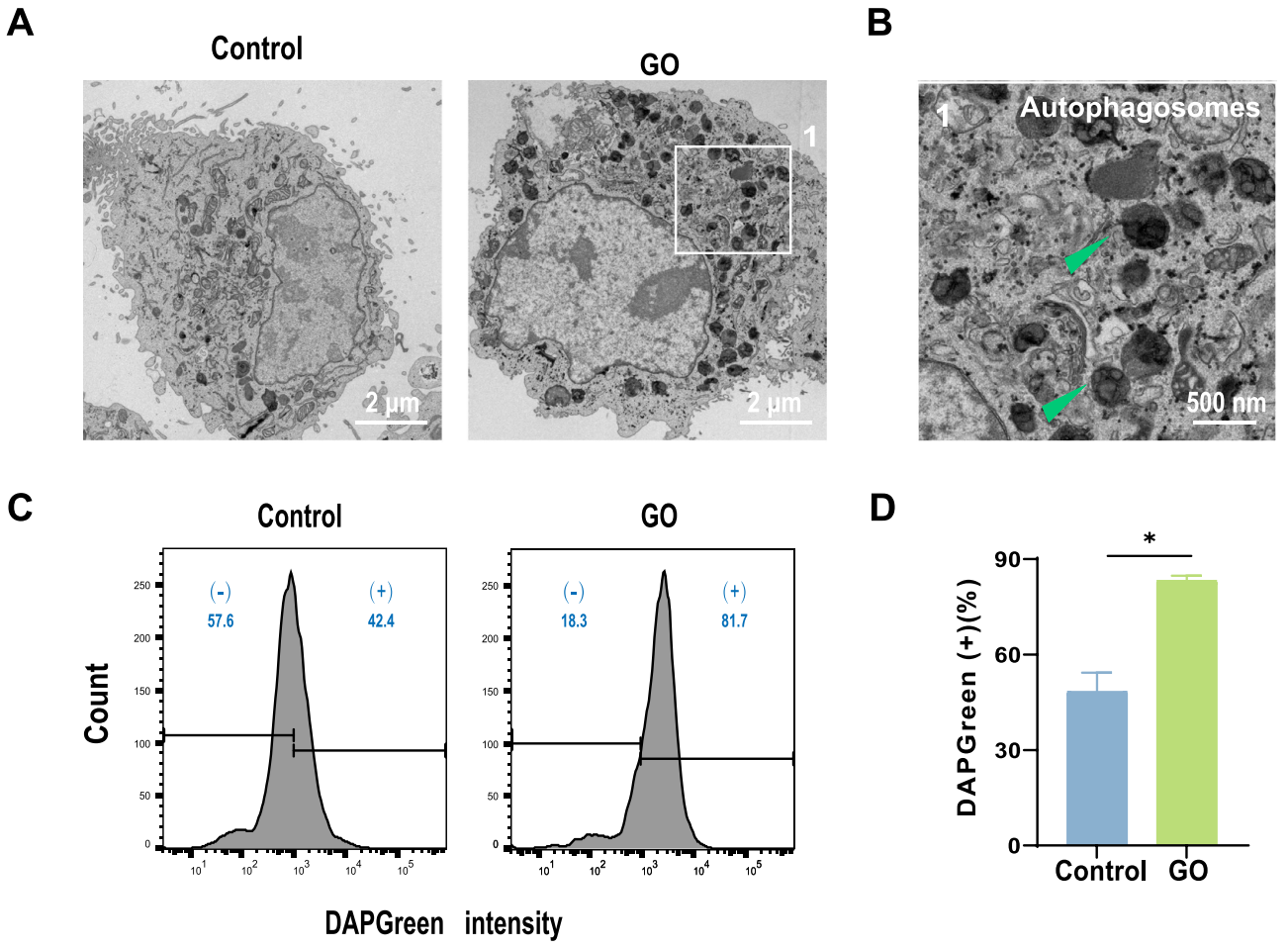

Figure 3 Autophagy induced by GO nanosheets in KGN cells. (**A**) Representative TEM images of KGN cells treated with and without GO nanosheets. (**B**) Enlarged image of autophagosomes represented by the white rectangles in A. (**C** and **D**) Autophagy intensity and quantification of GO-induced DAPGreen assays; (+) indicate DAPGreen (+) (%). Statistical differences between experimental groups were analyzed by the Student's *t*-test. *$p < 0.05$.

https://doi.org/10.2147/IJN.S495259

whether GO nanosheet treatment triggers autophagy, we quantitatively analyzed the level of autophagy after GO nanosheet treatment using the DAPGreen autophagosome detection probe. As shown in Figure 3C and D, the intensity of autophagy following GO nanosheet treatment was nearly double that of normal cells, suggesting that GO nanosheets do induce autophagy to eliminate damaged cells or mitochondria for survival.

GO Nanosheet Treatment Results in Mitochondrial Fragmentation

Mitochondrial damage typically manifests as changes in mitochondrial morphology and damage to the mitochondrial cristae.[51,52] Mitochondrial morphological changes are characterized by the loss of mitochondrial membrane structural integrity, membrane lysis, mitochondrial fragmentation, and mitochondrial cristae damage characterized by cristae breakage.[53] To gain a deeper understanding of the mitochondrial damage caused by GO interaction with mitochondria, we further investigated the morphological changes of mitochondria before and after GO nanosheet treatment. Cells were first treated with 1 μg/mL GO nanosheets for 72 h, stained with the commercial probe Mito-tracker Deep Red FM (MTDR), and then confocal fluorescence microscopy was used to capture morphological changes in mitochondria, allowing visualization of the effects of GO on mitochondria. As shown in Figure 4A, mitochondria exhibit different morphologies, with most of the mitochondria in normal cells being filamentous, while mitochondrial morphology in GO

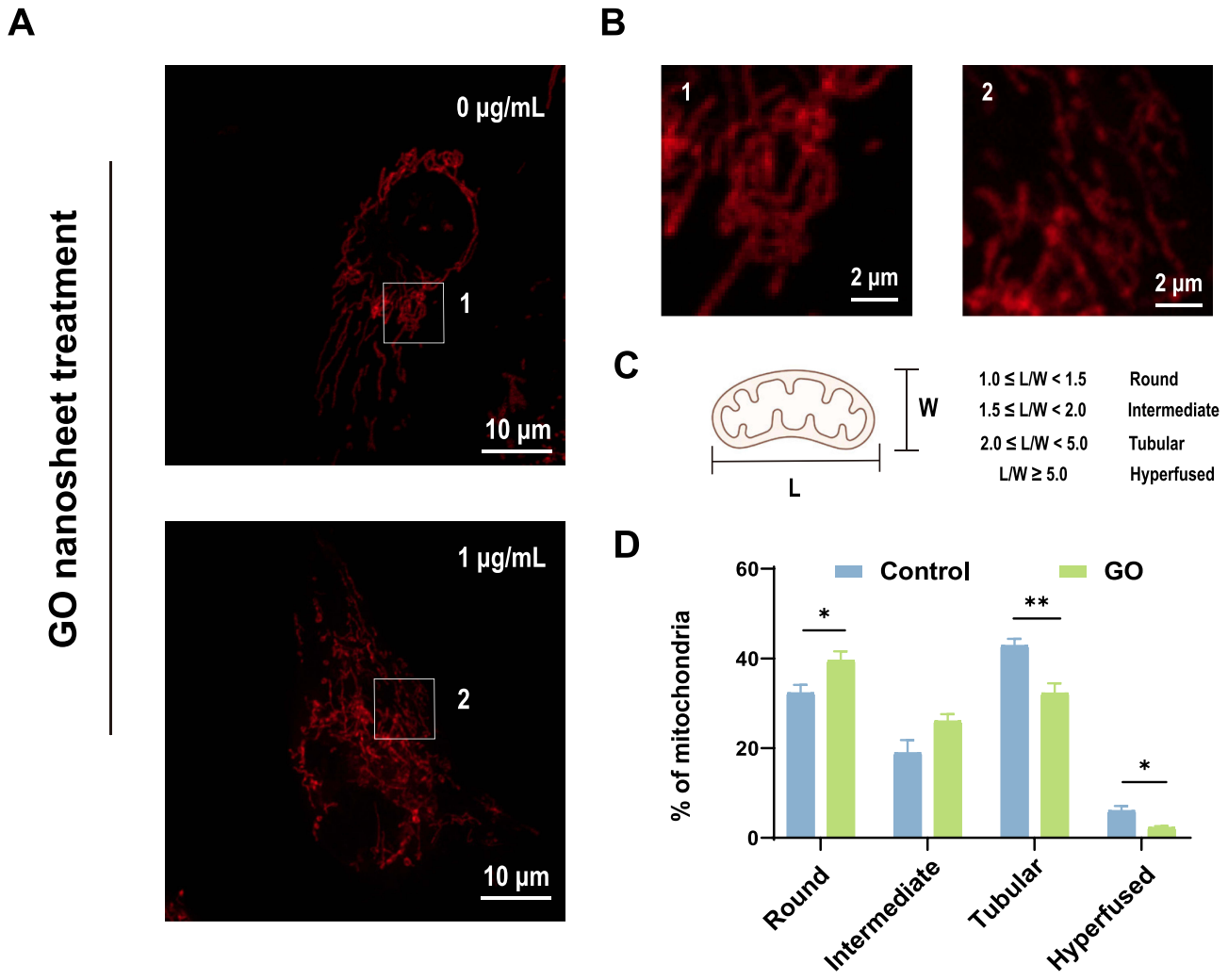

Figure 4 The damage to mitochondrial morphology induced by GO nanosheets in KGN cells. (**A**) Representative images of mitochondrial morphology of KGN cells treated with and without GO nanosheets. (**B**) Enlarged image of mitochondrial morphology represented by the white rectangles in A. (**C**) Depicts of mitochondrial morphology based on L/W distribution parameters. (**D**) The ratio of mitochondrial morphology quantitatively analyzed in A. Data in D are expressed as Mean ± SEM (n=5). Statistical differences between experimental groups were analyzed by the Student's *t*-test. *$p < 0.05$, **$p < 0.01$.

nanosheet-treated cells partially transformed into punctate structures (Figure 4B), suggesting that GO nanosheet treatment leads to mitochondrial breakage.

According to the previously reported protocol,[54,55] the length and width of mitochondria were analyzed, and the distribution of different mitochondrial morphologies was quantified by calculating the ratio of mitochondrial length and width (L/W). Mitochondrial morphology is divided into four categories based on L/W values (Figure 4C): round ($1.0 \leq L/W < 1.5$), intermediate ($1.5 \leq L/W < 2.0$), tubular ($2.0 \leq L/W < 5.0$), and hyperfused ($L/W \geq 5.0$).[56] We found that 1 μg/mL of GO nanosheet treatment increased the proportion of round and intermediate mitochondria and decreased the proportion of tubular and hyperfused mitochondria (Figure 4D). These findings undoubtedly suggest that the use of GO at concentrations greater than 1 μg/mL does cause serious damage to mitochondrial morphology. This finding is consistent with what we have observed with TEM (Figure 2).

GO Nanosheet Treatment Reduces Mitochondrial Function

The function of mitochondria is maintained by mitochondrial kinetic stability, ie, mitochondria undergo continuous fission and fusion.[43] Therefore, changes in mitochondrial morphology may cause mitochondrial dysfunction. GO has been reported to lead to cytotoxicity by inducing membrane damage, mitochondrial dysfunction, and ROS overproduction.[57] It has been reported that GO treatment may affect mitochondrial membrane potential (MMP) by inducing changes in mitochondrial morphology.[58] We hypothesize that GO nanosheet treatment causes mitochondrial dysfunction. To test this hypothesis, firstly, GO nanosheets were co-incubated with KGN cells for 72 h and the levels of MMP were assessed by Rhodamine 123 staining assay. From the results of Figure 5A and C, the fluorescence intensity of GO nanosheet-treated cells was reduced compared to cells without any treatment, suggesting that GO caused a decrease in MMP.

Mitochondria are organelles that provide energy to cells, studies have shown that mitochondria are the main site of ROS production[59] and that excess ROS production may lead to biomolecular damage, which in turn can lead to cell death.[60,61] The increased production of ROS, a byproduct of mitochondrial energy metabolism, will also lead to an increase in oxidative stress. Nanomaterials have been found to induce an increase in oxidative stress, which can negatively affect cells.[62–64] To explore the effect of GO nanosheets on ROS production in KGN cells, cells were treated with 1 μg/mL GO nanosheets for 72 h. Subsequently, the ROS level was detected using DCFH-DA staining. Confocal fluorescence microscopy showed that GO nanosheet-treated cells exhibited enhanced fluorescence intensity (Figure 5B and D), indicating an increase in intracellular ROS level following GO nanosheet treatment. This finding was further supported by quantitative analysis using a microplate reader (Figure S3), providing strong evidence that GO induces cell apoptosis by stimulating excessive ROS production.

To gain a more comprehensive understanding of GO-induced mitochondrial dysfunction and to further determine whether GO nanosheet treatment affected other mitochondrial functions, ATP production analysis was performed with and without GO nanosheet treatment. Quantitative analysis of ATP production showed that GO-treated cells exhibited significantly reduced ATP production compared to GO-untreated cells (Figure 5E).

Mitochondrial electron transport chain (ETC) coupled to oxidative phosphorylation. Mitochondrial ETC is divided into two respiratory chains depending on the hydrogen donor (NADH or $FADH_2$). However, studies have shown that ATP synthesis is only associated with NADH.[65] To further explore the underlying mechanism of GO reducing mitochondrial function, we investigated whether GO affects the activity of mitochondrial complexes. Complex I, as the most important and typical complex in the NADH respiratory chain, plays a crucial role in determining mitochondrial function.[66,67] Therefore, we hypothesize that GO may reduce mitochondrial function by affecting the activity of complex I. To test this hypothesis, we assessed the activity of complex I using the mitochondrial complex I enzymatic activity assay Kit (Abcam, Waltham, USA) to assess the effect of GO on mitochondrial complex activity. As shown in Figure 5F, the activity of complex I in the GO-treated cells was significantly reduced compared to normal cells.

Mitochondria are the main energy providers within the cells, and the normal opening of the mPTP and the integrity of the membrane are necessary to maintain the membrane potential and energy metabolism of the mitochondria.[68] The fluorescent reagent calcein-AM is passively transported into cells and aggregates in the cytoplasm and mitochondria,[69] resulting in strong green fluorescence (Figure 5G). Under normal physiological pH conditions, mPTP does not open so

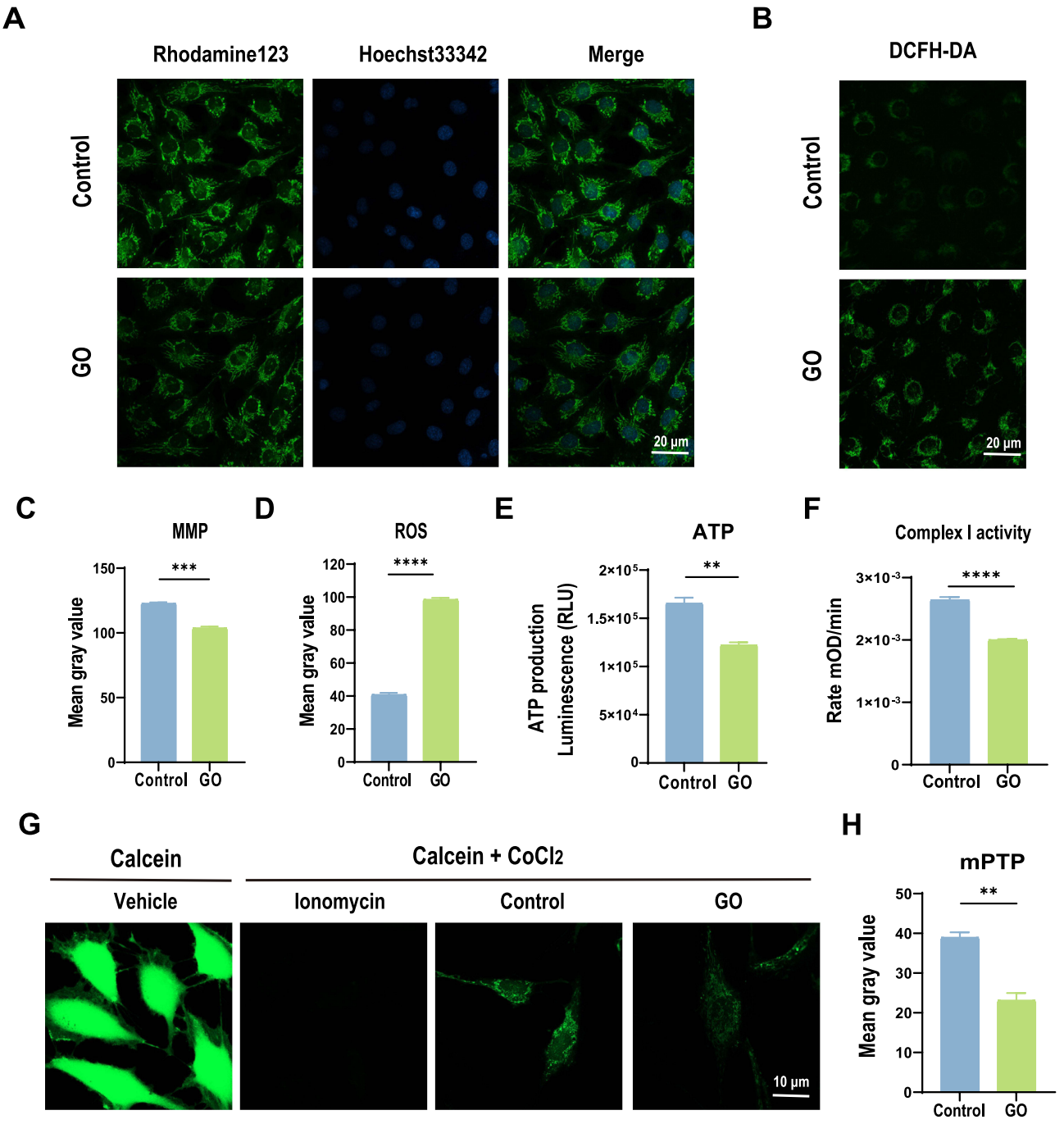

Figure 5 Mitochondrial functional damage induced by GO nanosheets in KGN cells. (**A** and **C**) GO nanosheets reduced MMP in KGN cells, while quantitative analysis was shown in C. (**B** and **D**) Representative images of GO nanosheets increasing intracellular ROS levels in KGN cells, while quantitative analysis was shown in D. (**E**) GO nanosheets reduced the level of ATP produced by mitochondria in KGN cells. (**F**) GO nanosheets reduced the enzymatic activity of mitochondrial complex I in KGN cells. (**G** and **H**) GO nanosheets induced the opening of the mitochondrial permeability transition pore (mPTP) in KGN cells. Data are expressed as Mean ± SEM (n=3), and statistical differences between experimental groups were analyzed by the Student's *t*-test. $^{**}p < 0.01$, $^{***}p < 0.001$ and $^{****}p < 0.0001$.

that the fluorescent quenchant $CoCl_2$ cannot enter the mitochondria, thus showing green fluorescence only in the mitochondria. As a positive control, further treatment with the calcium ionophore Ionomycin induces a large amount of extracellular Ca^{2+} into the intracellular and mitochondrial matrix and induces mPTP opening, resulting in almost total quenching of intracellular green fluorescence. The data in Figure 5C showed that the GO nanosheet treatment group reduced the mitochondrial membrane potential by 20% compared to the control group, possibly due to GO-induced abnormal opening of mPTP. To further explore the underlying mechanism of GO leading to the reduction of MMP, we

investigated whether GO affects mPTP. We observed that GO exposure for 72h led to a decrease in fluorescence intensity within mitochondria (Figure 5H). This suggests that GO exposure leads to mPTP opening, which further alters mitochondrial permeability. This may increase the level of cellular stress and accelerate the process of apoptosis. This result is also consistent with previous studies.[70]

Mitochondrial Dysfunction Due to Short-Term GO Exposure Is Reversible

Previous studies have shown that short-term GO exposure results in acute toxicity, such as cell death.[16] Therefore, we hypothesize that the mitochondrial damage caused by short-term GO exposure is an acute injury caused by cellular stress and that the damaged mitochondria may gradually return to normal when the cells leave the GO exposure environment. To test this hypothesis, we further investigated the changes in mitochondrial function after the cells left the GO-exposed environment. We first incubated 1 μg/mL of GO nanosheets with KGN cells for 72 h. After incubation, cells in both GO-treated and untreated groups were thoroughly washed with PBS and seeded into new cell culture plates. Mitochondrial function, including ATP production, intracellular ROS content, and MMP, was determined on the third and seventh days. As shown in Figure 6A–C, we observed that the cells in the GO treatment group still had mitochondrial dysfunction on the third day, such as reduced ATP production, excessive ROS accumulation, and decreased MMP. However, it is worth noting that the ATP production and intracellular ROS levels in the GO treatment group gradually approached those of normal cells, suggesting that mitochondrial function was gradually restored in the GO treatment group. This suspicion was confirmed in the mitochondrial function assay on day 7. We found that mitochondrial function returned to normal on day 7 after KGN cells left the GO-exposed environment. There were no differences in ATP production, intracellular ROS levels, and MMP levels between GO-exposed and normal cells (as shown in Figure 6A, B and D).

Discussions

In recent years, with the continuous development of biomedical applications of nanomaterials, nanotoxicity has gradually attracted widespread attention.[46,71] Determining the penetration and retention of nanomaterials in different cells or tissues is critical in nanotoxicity studies. At present, the toxicity of nanomaterials to various cell lines and animal models has been well studied, however, the study of nanomaterials on the human reproductive system at the subcellular level has been largely neglected. Graphene Oxide is becoming more widely used in the field of reproductive medicine, however, its toxicity to the human reproductive system at the cellular and subcellular levels has not been effectively assessed. Therefore, we investigated the cytotoxicity and mitochondrial toxicity of GO nanosheets on the human ovarian granulosa cell line KGN to explore GO-induced female reproductive toxicity.

In this study, we first explored the toxic effects of GO nanosheets on the human ovarian granulosa cell line KGN through a cell viability assay. KGN cells were treated with different concentrations of GO nanosheets ranging from 0.1 to 100 μg/mL, and we found that GO promoted its cytotoxic effects in a time- and dose-dependent manner. Low doses (0.1 and 1 μg/mL) of GO nanosheets that were considered to be far from lethal concentrations were used in this experiment. Interestingly, cell viability was significantly reduced in the GO-treated group at a concentration of 0.1 μg/mL compared to the untreated group. Several studies on the in vitro toxicity of nanoparticles have shown that there are differences in the thresholds at which different types of nanomaterials lead to different types of cytotoxicity. For example, although 0.5 μg/mL multi-walled carbon nanotubes did not cause significant damage to the spermatogonial cell line GC-2 spd cells, their accumulation in mitochondria was detected.[72] A study investigating the reproductive toxicity of GO in boars showed that doses above 5 μg/mL were toxic to spermatocytes (reduced viability, fertilization ability), but low doses of 1 μg/mL promoted sperm fertilization ability.[73] A toxicity study of Ag-NP on bovine ovarian granulosa cells showed that granulosa cell viability was significantly impaired after 24 h exposure to Ag-NP at doses greater than 5 μg/mL. However, Ag-NP did not cause significant damage to ovarian granulosa cells at a dose of 1 μg/mL.[74] These findings may be related to differences in nanomaterial characteristics and cell phenotypes. In conclusion, KGN cells showed higher sensitivity to GO, which may cause impairment of reproductive function at low doses. Considering that GO exposure in realistic scenarios (occupational or clinical scenarios) may be continuous, it is recommended to further explore whether long-term bioaccumulation of GO in vivo causes chronic or irreversible damage to human reproductive health.

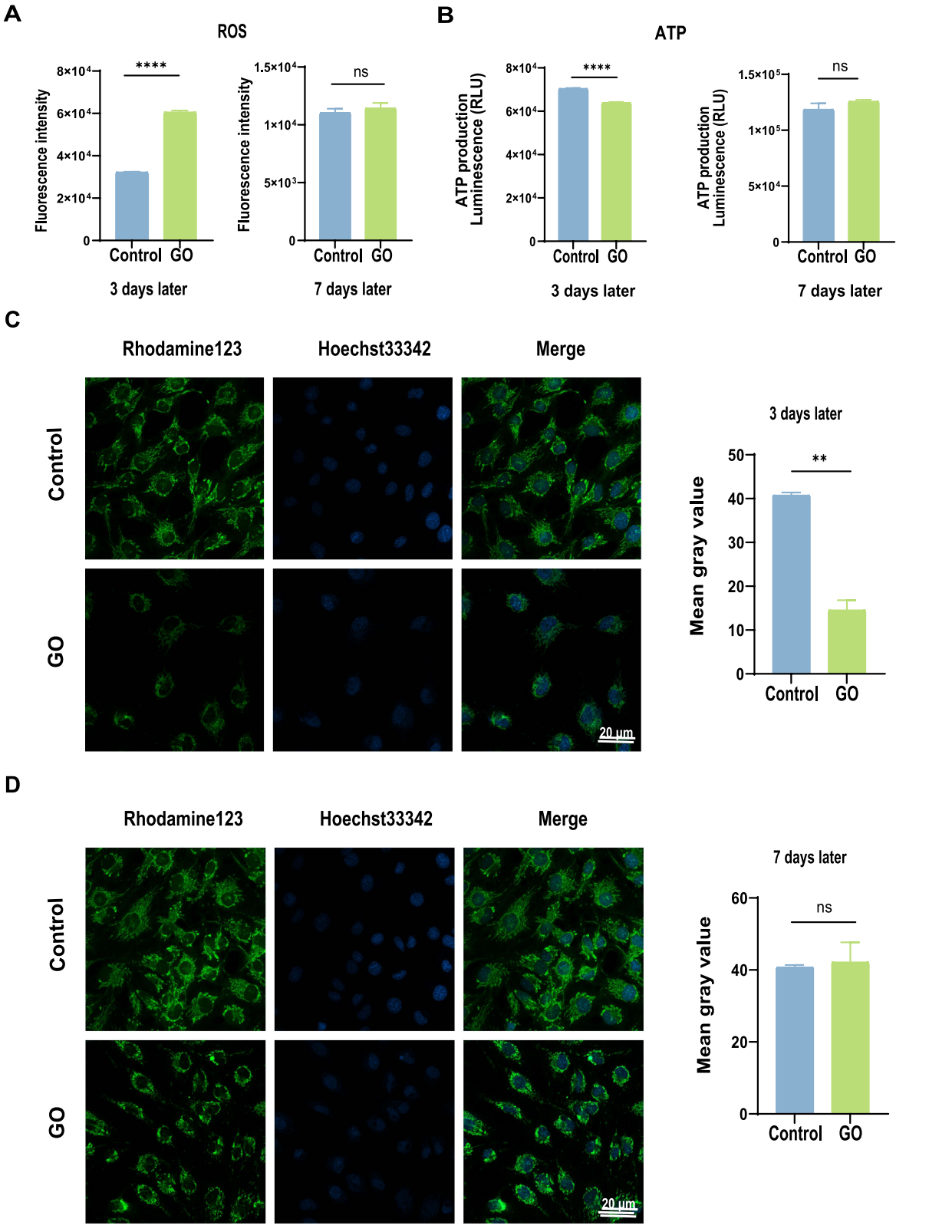

Figure 6 Mitochondrial function gradually returned to normal after KGN left the GO nanosheet-exposed environment. (**A**) ROS levels of KGN cells on days 3 and 7 after leaving the GO-exposed environment. (**B**) ATP levels of KGN cells on days 3 and 7 after leaving the GO-exposed environment. (**C**) MMP levels of KGN cells on days 3 after leaving the GO-exposed environment. (**D**) MMP levels of KGN cells on days 7 after leaving the GO-exposed environment. Data are expressed as Mean ± SEM (n=3), and statistical differences between experimental groups were analyzed by the Student's *t*-test. $^{**}p < 0.01$ and $^{****}p < 0.0001$.

Mitochondrial metabolic processes such as oxidative phosphorylation produce ROS,[75] and cellular redox bias caused by increased ROS may eventually trigger apoptosis.[34] In this study, the results of DCFH-DA staining showed an increase in ROS in KGN cells in the GO nanosheet treatment group compared to the control group, demonstrating that GO nanosheet treatment resulted in excessive ROS production in the cells and induced apoptosis in KGN. This is consistent with the FITC-Annexin V/PI results showing an increase in the number of apoptotic cells in the GO nanosheet-treated group (Figure 1B and C). According to a recent study, GO-induced increase in ROS in neuroblastoma cells reduces cellular antioxidant capacity mainly through activation of the NADPH oxidase 2 (NOX 2) signaling pathway.[34] However, GO-induced ROS increases in different cell types may be through different mechanisms or molecular pathways. Further studies are needed on the intrinsic mechanism of GO-induced ROS overproduction in ovarian granulosa cells. It has been reported that excessive ROS may affect ovarian granulosa cell functions such as steroidogenesis, hormone signaling, and oocyte maturation, and ultimately negatively impact reproductive outcomes.[76] To avoid adverse effects on female reproductive health, it is crucial to further understand the mechanisms by which GO induces ROS overproduction in ovarian granulosa cells.

GO has been reported to disrupt membrane integrity by enhancing its ability to interfere with membranes.[77] GO nanosheets triggered lipid peroxidation during adhesion to cell surface membranes,[34] and the overproduction of ROS might be the first step in oxidative stress. Therefore, the microdamage of the mitochondrial membrane caused by GO nanosheet treatment in this study could also be due to the overproduction of ROS. It leads to mitochondrial dysfunction by destroying the integrity of the mitochondrial membrane, which leads to KGN cell apoptosis. In terms of GO-induced mitochondrial membrane damage, Wang et al have reported that small GO nanosheets can be inserted into biological membranes,[78,79] and our previous study showed that GO nanosheets are most likely to cause membrane damage by "cutting" the mitochondrial membrane.[80]

As previously reported, excessive opening of mPTP leads to increased mitochondrial permeability and translocation of pro-apoptotic factors from mitochondria to cytoplasm, which further activates endogenous apoptotic pathways in mitochondria.[34,81] Regulation of apoptosis by endogenous mitochondrial pathways has also been reported in other types of nanomaterials such as zinc oxide, cuprous oxide, and silica nanoparticles.[82–84] In this study, GO exposure leading to mPTP opening may have induced mitochondrial stress, which in turn led to KGN cell apoptosis. The specific mechanism needs to be further explored. However, mitochondrial stress does not always lead to apoptosis and may also stimulate autophagy to remove damaged mitochondria and prevent further cell damage. The above conjecture was also verified by the observation of increased autophagosomes in the cells of the GO-treated group using the DAPGreen autophagosome detection probe and TEM. It has been reported that cells can regulate autophagy by influencing AMPK and mTORC1 signaling to sense energy changes.[85] This suggests a potential link between mitochondrial dysfunction, such as reduced ATP production, and autophagy. However, the specific mechanism by which GO induces KGN autophagy remains unclear. In addition, autophagy under physiological conditions has been reported to contribute to the maintenance of healthy primordial follicle numbers and germ cell survival. However, excessive autophagy can alter the quality and quantity of oocytes, ultimately causing adverse effects on female reproductive health.[86] This suggests that excessive levels of autophagy in ovarian granulosa cells may also affect oocyte maturation, leading to female reproductive dysfunction. Therefore, the detailed mechanisms by which GO leads to enhanced autophagy in ovarian granulosa cells and its effects on female reproductive health warrant further investigation. This may require validation in animal models.

In summary, our study demonstrated that GO nanosheets induced mitochondrial damage in human ovarian granulosa cells, including mitochondrial breakage, mitochondrial dysfunction, and ultimately cell death, even at low concentrations within the generally accepted safe concentration range. However, due to the limitations of the ovarian granulosa cell line KGN, it might not fully represent the physiological responses to GO exposure in human ovarian granulosa cells and in vivo. Therefore, it is necessary to further explore the cellular and mitochondrial toxicity induced by GO in primary ovarian granulosa cells or oocytes and its molecular mechanisms. In addition, our study suggests that single-dose GO treatment leads to reversible mitochondrial damage in the short term. However, given the high sensitivity of the ovary to nanoparticles or invasive substances, transient mitochondrial dysfunction and ovarian granulosa cell apoptosis may also negatively affect female reproductive function, including follicular atresia, and impaired oocyte maturation. This needs further validation in animal models. However, in real-life scenarios or clinical scenarios, GO exposure is a long-term

ongoing process. Thus, damage to ovarian granulosa cells and mitochondria by repeated doses of GO long-term exposure is a continuous process. Whether this causes permanent mitochondrial damage and leads to female reproductive dysfunction, such as infertility, remains unclear. Further validation in animal models is necessary regarding mitochondrial damage and female reproductive dysfunction caused by single-dose short-term exposure and repeated-dose long-term exposure to GO. GO-based biomedical applications require further toxicity studies to find a clearer safety window, as GO-induced ovarian granulosa cell death can negatively affect female reproductive function.

Conclusion

In summary, a single dose of GO exposure for 72 h resulted in the death of KGN cells in a dose-dependent manner and led to reversible damage (acute damage) to mitochondrial structure and function, such as abnormalities in membrane structure and mitochondrial cristae, mitochondrial fragmentation, reduced ATP production, excessive ROS accumulation, and reduced MMP. Mitochondrial dysfunction caused by short-term GO exposure gradually recovered after leaving the GO-exposed environment. However, transient damage to ovarian granulosa cells may have caused irreversible damage to ovarian reserve function. This needs to be further verified in animal experiments. Therefore, it is recommended to further investigate the cellular and mitochondrial toxicity induced by repeated doses of GO for short-term exposures (within a few hours or 72 hours) or long-term exposures (days or weeks) and their possible mechanisms. Validation in animal models will further elucidate the short- or long-term effects of GO exposure in vivo on mitochondrial or reproductive function. Given that mitochondrial dysfunction is associated with a wide range of diseases, our study demonstrates the importance of mitochondrial health in exploring the toxicological effects and broad cellular functions of nanomaterials. In addition, our findings fill an important gap in the female reproductive toxicity of GO, which is critical for evaluating its safety in female reproductive health applications. Therefore, the safe dose range of GO for biomedical applications needs to be further explored and investigated, especially in human reproductive health.

Ethics Approval

The research protocol related to the human ovarian granulosa cell line KGN in this study was approved by the Ethics Committee of Anhui Medical University (20170046). All methods were carried out in strict accordance with the relevant guidelines and regulations.

Acknowledgment

The authors thank the Center for Scientific Research of Anhui Medical University for their valuable help in our experiment.

Author Contributions

All authors made a significant contribution to the work reported, whether that is in the conception, study design, execution, acquisition of data, analysis, and interpretation, or in all these areas; took part in drafting, revising or critically reviewing the article; gave final approval of the version to be published; have agreed on the journal to which the article has been submitted; and agree to be accountable for all aspects of the work.

Funding

This research was funded by the National Key R&D Program of China, grant number 2024YFC2707200; the National Natural Science Foundation of China, grant number 82001635; the Hefei Comprehensive National Science Center Medical-Industrial Integration Medical Equipment Innovation Research Platform Project, grant number 4801001202; the Clinical Medical Research Transformation Project of Anhui Province, grant number 202204295107020012; the Foundation for Selected Scientists Studying Abroad of Anhui Province, grant number 2022LCX015; Postgraduate Innovation Research and Practice Program of Anhui Medical University, grant number YJS20230186; and the Innovation and Entrepreneurship Training Program for Undergraduate Students of Anhui Medical University, grant number 202310366015, S202310366009.

Disclosure

The authors report no conflicts of interest in this work.

References

1. Novoselov KS, Geim AK, Morozov SV, et al. Electric field effect in atomically thin carbon films. *Science*. 2004;306(5696):666–669. doi:10.1126/science.1102896
2. Chen D, Feng H, Li J. Graphene oxide: preparation, functionalization, and electrochemical applications. *Chem Rev*. 2012;112(11):6027–6053. doi:10.1021/cr300115g
3. Li R, Mansukhani ND, Guiney LM, et al. Identification and optimization of carbon radicals on hydrated graphene oxide for ubiquitous antibacterial coatings. *ACS Nano*. 2016;10(12):10966–10980. doi:10.1021/acsnano.6b05692
4. Mennel L, Symonowicz J, Wachter S, Polyushkin DK, Molina-Mendoza AJ, Mueller T. Ultrafast machine vision with 2D material neural network image sensors. *Nature*. 2020;579(7797):62–66. doi:10.1038/s41586-020-2038-x
5. Liu X, Yan B, Li Y, et al. Graphene oxide-grafted magnetic nanorings mediated magnetothermodynamic therapy favoring reactive oxygen species-related immune response for enhanced antitumor efficacy. *ACS Nano*. 2020;14(2):1936–1950. doi:10.1021/acsnano.9b08320
6. Zheng XT, Ananthanarayanan A, Luo KQ, Chen P. Glowing graphene quantum dots and carbon dots: properties, syntheses, and biological applications. *Small*. 2015;11(14):1620–1636. doi:10.1002/smll.201402648
7. Xu C, Hong H, Lee Y, et al. Efficient lymph node-targeted delivery of personalized cancer vaccines with reactive oxygen species-inducing reduced graphene oxide nanosheets. *ACS Nano*. 2020;14(10):13268–13278. doi:10.1021/acsnano.0c05062
8. Yaghoubi F, Motlagh NSH, Naghib SM, Haghiralsadat F, Jaliani HZ, Moradi A. A functionalized graphene oxide with improved cytocompatibility for stimuli-responsive co-delivery of curcumin and doxorubicin in cancer treatment. *Sci Rep*. 2022;12(1):1959. doi:10.1038/s41598-022-05793-9
9. Mohammadi A, Koruji M, Azami M, et al. Polycaprolactone/testicular extracellular matrix/graphene oxide-based electrospun tubular scaffolds for reproductive medicine: biomimetic architecture of seminiferous tubules. *Macromol Biosci*. 2023;24(2):e2300342. doi:10.1002/mabi.202300342
10. Bernabo N, Valbonetti L, Raspa M, et al. Graphene oxide improves in vitro fertilization in mice with no impact on embryo development and preserves the membrane microdomains architecture. *Front Bioeng Biotechnol*. 2020;8:629. doi:10.3389/fbioe.2020.00629
11. Amrollahi-Sharifabadi M, Koohi MK, Zayerzadeh E, Hablolvarid MH, Hassan J, Seifalian AM. In vivo toxicological evaluation of graphene oxide nanoplatelets for clinical application. *Int J Nanomed*. 2018;13:4757–4769. doi:10.2147/ijn.S168731
12. Park E-J, Lee SJ, Lee K, et al. Pulmonary persistence of graphene nanoplatelets may disturb physiological and immunological homeostasis. *J Appl Toxicol*. 2017;37(3):296–309. doi:10.1002/jat.3361
13. Erf GF, Falcon DM, Sullivan KS, Bourdo SE. T lymphocytes dominate local leukocyte infiltration in response to intradermal injection of functionalized graphene-based nanomaterial. *J Appl Toxicol*. 2017;37(11):1317–1324. doi:10.1002/jat.3492
14. Xu M, Zhu J, Wang F, et al. Improved in vitro and in vivo biocompatibility of graphene oxide through surface modification: poly(acrylic acid)-functionalization is superior to PEGylation. *ACS Nano*. 2016;10(3):3267–3281. doi:10.1021/acsnano.6b00539
15. Mao L, Hu M, Pan B, Xie Y, Petersen EJ. Biodistribution and toxicity of radio-labeled few layer graphene in mice after intratracheal instillation. *Part Fibre Toxicol*. 2016;13(1):7. doi:10.1186/s12989-016-0120-1
16. Mohamed HRH, Welson M, Yaseen AE, El-Ghor A. Induction of chromosomal and DNA damage and histological alterations by graphene oxide nanoparticles in Swiss mice. *Drug Chem Toxicol*. 2019;44(6):631–641. doi:10.1080/01480545.2019.1643876
17. Chwalibog A, Sawosz E, Jaworski S, et al. Toxicity of pristine graphene in experiments in a chicken embryo model. *Int J Nanomed*. 2014;9:3913–3922. doi:10.2147/ijn.S65633
18. Jaworski S, Strojny B, Sawosz E, et al. Degradation of mitochondria and oxidative stress as the main mechanism of toxicity of pristine graphene on U87 glioblastoma cells and tumors and HS-5 cells. *Int J Mol Sci*. 2019;20(3):650. doi:10.3390/ijms20030650
19. Gurunathan S, Arsalan Iqbal M, Qasim M, et al. Evaluation of graphene oxide induced cellular toxicity and transcriptome analysis in human embryonic kidney cells. *Nanomaterials*. 2019;9(7):969. doi:10.3390/nano9070969
20. Zheng P, Ding B, Jiang Z, et al. Ultrasound-augmented mitochondrial calcium ion overload by calcium nanomodulator to induce immunogenic cell death. *Nano Lett*. 2021;21(5):2088–2093. doi:10.1021/acs.nanolett.0c04778
21. Wai T, Langer T. Mitochondrial dynamics and metabolic regulation. *Trends Endocrinol Metab*. 2016;27(2):105–117. doi:10.1016/j.tem.2015.12.001
22. Sabouny R, Shutt TE. Reciprocal regulation of mitochondrial fission and fusion. *Trends Biochem Sci*. 2020;45(7):564–577. doi:10.1016/j.tibs.2020.03.009
23. Nunnari J, Suomalainen A. Mitochondria: in sickness and in health. *Cell*. 2012;148(6):1145–1159. doi:10.1016/j.cell.2012.02.035
24. Baughman JM, Perocchi F, Girgis HS, et al. Integrative genomics identifies MCU as an essential component of the mitochondrial calcium uniporter. *Nature*. 2011;476(7360):341–345. doi:10.1038/nature10234
25. MurphyMichael P. How mitochondria produce reactive oxygen species. *Biochem J*. 2008;417(1):1–13. doi:10.1042/bj20081386
26. Lu Y, Li Z, Zhang S, Zhang T, Liu Y, Zhang L. Cellular mitophagy: mechanism, roles in diseases and small molecule pharmacological regulation. *Theranostics*. 2023;13(2):736–766. doi:10.7150/thno.79876
27. Ma K, Chen G, Li W, Kepp O, Zhu Y, Mitophagy CQ. Mitochondrial homeostasis, and cell fate. *Front Cell Develop Biol*. 2020;8:467. doi:10.3389/fcell.2020.00467
28. Bhardwaj JK, Bikal P, Sachdeva SN. Cadmium as an ovarian toxicant: a review. *J Appl Toxicol*. 2023;44(1):129–147. doi:10.1002/jat.4526
29. Bhardwaj JK, Bikal P, Sachdeva SN. Chemotherapeutic drugs induced female reproductive toxicity and treatment strategies. *J Biochem Mol Toxicol*. 2023;37(7):e23371. doi:10.1002/jbt.23371
30. Lopes F, Smith R, Anderson RA, Spears N. Docetaxel induces moderate ovarian toxicity in mice, primarily affecting granulosa cells of early growing follicles. *Mol Hum Reprod*. 2014;20(10):948–959. doi:10.1093/molehr/gau057
31. Canipari R. Oocyte–granulosa cell interactions. *Hum Reprod Update*. 2000;6(3):279–289. doi:10.1093/humupd/6.3.279
32. Bhardwaj JK, Sharma RK. Scanning electron microscopic changes in granulosa cells during follicular atresia in Caprine ovary. *Scanning*. 2011;33(1):21–24. doi:10.1002/sca.20217

33. Sreerangaraja Urs DB, Wu W-H, Komrskova K, et al. Mitochondrial function in modulating human granulosa cell steroidogenesis and female fertility. *Int J Mol Sci*. 2020;21(10):3592. doi:10.3390/ijms21103592
34. Xiaoli F, Yaqing Z, Ruhui L, et al. Graphene oxide disrupted mitochondrial homeostasis through inducing intracellular redox deviation and autophagy-lysosomal network dysfunction in SH-SY5Y cells. *J Hazard Mater*. 2021;416:126158. doi:10.1016/j.jhazmat.2021.126158
35. Hong Q, Fan M, Cai R, et al. SOX4 regulates proliferation and apoptosis of human ovarian granulosa-like tumor cell line KGN through the Hippo pathway. *Biochem Biophys Res Commun*. 2024;705:149738. doi:10.1016/j.bbrc.2024.149738
36. Wang W, Zhou C, Ma Z, et al. Co-exposure to polystyrene nanoplastics and triclosan induces synergistic cytotoxicity in human KGN granulosa cells by promoting reactive oxygen species accumulation. *Ecotoxicol Environ Saf*. 2024;273:116121. doi:10.1016/j.ecoenv.2024.116121
37. Qiu K, Zou W, Fang Z, et al. 2D MoS2 and BN nanosheets damage mitochondria through membrane penetration. *ACS Nano*. 2023;17 (5):4716–4728. doi:10.1021/acsnano.2c11003
38. Zhao X, Zhao C, Wang Y, et al. Cytotoxicity of graphene oxide and graphene oxide loaded with doxorubicin on human multiple myeloma cells. *Int J Nanomed*. 2014;9:1413–1421. doi:10.2147/ijn.S57946
39. Ajayi BE, Oboh B, Minari JB, Sexton DW, Sarker SD, Fatokun AA.Cola rostrata K. Schum. constituents induce cytotoxicity through reactive oxygen species generation and mitochondrial membrane depolarisation. *Exploration of Targeted Anti-Tumor Therapy*. 2023;4(6):1328–1344. doi:10.37349/etat.2023.00200
40. Yang Z, Shi H, Chinnathambi A, et al. Arbutin exerts anticancer activity against rat C6 glioma cells by inducing apoptosis and inhibiting the inflammatory markers and P13/Akt/mTOR cascade. *J Biochem Mol Toxicol*. 2021;35(9):e22857. doi:10.1002/jbt.22857
41. You F, Li Q, Jin G, Zheng Y, Chen J, Yang H. Genistein protects against Aβ25–35 induced apoptosis of PC12 cells through JNK signaling and modulation of Bcl-2 family messengers. *BMC Neuro*. 2017;18(1):12. doi:10.1186/s12868-016-0329-9
42. Wan M, Wang C, Cui J, Xia Q, Zhang L. Silencing KLF6 alleviates cigarette smoke extract-induced mitochondrial dysfunction in bronchial epithelial cells by SIRT4 upregulation. *Int J Chronic Obstr*. 2024;19:815–828. doi:10.2147/copd.S451264
43. Qiu K, Zou W, Fang H, et al. Light-activated mitochondrial fission through optogenetic control of mitochondria-lysosome contacts. *Nat Commun*. 2022;13(1):4303. doi:10.1038/s41467-022-31970-5
44. Fusco L, Orecchioni M, Reina G, et al. Lateral dimension and amino-functionalization on the balance to assess the single-cell toxicity of graphene on fifteen immune cell types. *NanoImpact*. 2021;23:100330. doi:10.1016/j.impact.2021.100330
45. Hadrup N, Sahlgren N, Jacobsen NR, et al. Toxicity dose descriptors from animal inhalation studies of 13 nanomaterials and their bulk and ionic counterparts and variation with primary particle characteristics. *Nanotoxicology*. 2023;17(4):338–371. doi:10.1080/17435390.2023.2221728
46. Krishnakumar S, Malavika RN, Nair SV, Menon D, Paul-Prasanth B. Nano-graphene oxide particles induce inheritable anomalies through altered gene expressions involved in oocyte maturation. *Nanotoxicology*. 2024;18(2):160–180. doi:10.1080/17435390.2024.2325615
47. Akhavan O. Graphene scaffolds in progressive nanotechnology/stem cell-based tissue engineering of the nervous system. *J Mat Chem B*. 2016;4 (19):3169–3190. doi:10.1039/c6tb00152a
48. Akhavan O. Bacteriorhodopsin as a superior substitute for hydrazine in chemical reduction of single-layer graphene oxide sheets. *Carbon*. 2015;81:158–166. doi:10.1016/j.carbon.2014.09.044
49. Dutta T, Sarkar R, Pakhira B, et al. ROS generation by reduced graphene oxide (rGO) induced by visible light showing antibacterial activity: comparison with graphene oxide (GO). *RSC Adv*. 2015;5(98):80192–80195. doi:10.1039/c5ra14061g
50. Bock FJ, Tait SWG. Mitochondria as multifaceted regulators of cell death. *Nat Rev Mol Cell Biol*. 2020;21(2):85–100. doi:10.1038/s41580-019-0173-8
51. Senyilmaz D, Virtue S, Xu X, et al. Regulation of mitochondrial morphology and function by stearoylation of TFR1. *Nature*. 2015;525 (7567):124–128. doi:10.1038/nature14601
52. Schapira AH. Mitochondrial disease. *Lancet*. 2006;368(9529):70–82. doi:10.1016/S0140-6736(06)68970-8
53. Yu T, Robotham JL, Yoon Y. Increased production of reactive oxygen species in hyperglycemic conditions requires dynamic change of mitochondrial morphology. *Proc Natl Acad Sci U S A*. 2006;103(8):2653–2658. doi:10.1073/pnas.0511154103
54. Shao XT, Chen QX, Hu LT, et al. Super-resolution quantification of nanoscale damage to mitochondria in live cells. *Nano Res*. 2020;13 (8):2149–2155. doi:10.1007/s12274-020-2822-9
55. Liu Y, Zhang C, Wei Y, et al. De Novo-Designed landmine warfare strategy luminophore for super-resolution imaging reveal ONOO– evolution in living cells. *Chem Eng J*. 2021;422:130151. doi:10.1016/j.cej.2021.130151
56. Wei YC, Kong LX, Chen HM, et al. Super-resolution image-based tracking of drug distribution in mitochondria of a label-free naturally derived drug molecules. *Chem Eng J*. 2022;429:132134. doi:10.1016/j.cej.2021.132134
57. Georgieva M, Vasileva B, Speranza G, et al. Amination of graphene oxide leads to increased cytotoxicity in hepatocellular carcinoma cells. *Int J Mol Sci*. 2020;21(7):2427. doi:10.3390/ijms21072427
58. Lammel T, Boisseaux P, Fernandez-Cruz ML, Navas JM. Internalization and cytotoxicity of graphene oxide and carboxyl graphene nanoplatelets in the human hepatocellular carcinoma cell line Hep G2. *Part Fibre Toxicol*. 2013;10:27. doi:10.1186/1743-8977-10-27
59. Ma X, Zhang L-H, Wang L-R, et al. Single-walled carbon nanotubes alter cytochrome c electron transfer and modulate mitochondrial function. *ACS Nano*. 2012;6(12):10486–10496. doi:10.1021/nn302457v
60. Tian X, Sun Y, Fan S, et al. Photogenerated charge carriers in molybdenum disulfide quantum dots with enhanced antibacterial activity. *ACS Appl Mater Interfaces*. 2019;11(5):4858–4866. doi:10.1021/acsami.8b19958
61. Tian X, Jiang X, Welch C, et al. Bactericidal effects of silver nanoparticles on lactobacilli and the underlying mechanism. *ACS Appl Mater Interfaces*. 2018;10(10):8443–8450. doi:10.1021/acsami.7b17274
62. Tee JK, Ong CN, Bay BH, Ho HK, Leong DT. Oxidative stress by inorganic nanoparticles. *Wiley Interdiscip Rev Nanomed Nanobiotechnol*. 2016;8 (3):414–438. doi:10.1002/wnan.1374
63. Loutfy SA, Salaheldin TA, Ramadan MA, Farroh Kh Y, Abdallah ZF, Youssef T. Synthesis, characterization and cytotoxic evaluation of graphene oxide nanosheets: in vitro liver cancer model. *Asian Pac J Cancer Prev*. 2017;18(4):955–961. doi:10.22034/APJCP.2017.18.4.955
64. Pelin M, Fusco L, Leon V, et al. Differential cytotoxic effects of graphene and graphene oxide on skin keratinocytes. *Sci Rep*. 2017;7:40572. doi:10.1038/srep40572
65. Guo R, Gu J, Zong S, Wu M, Yang M. Structure and mechanism of mitochondrial electron transport chain. *Biomedical J*. 2018;41(1):9–20. doi:10.1016/j.bj.2017.12.001

66. Cai X, Ng CP, Jones O, et al. Lactate activates the mitochondrial electron transport chain independently of its metabolism. *Molecular Cell*. 2023;83 (21):3904–3920.e7. doi:10.1016/j.molcel.2023.09.034
67. Spinelli JB, Rosen PC, Sprenger H-G, et al. Fumarate is a terminal electron acceptor in the mammalian electron transport chain. *Science*. 2021;374 (6572):1227–1237. doi:10.1126/science.abi7495
68. Tsutsumi K, Sasase T. Cellular calcification induced by inorganic polyphosphate involves ATP depletion and opening of the mitochondrial permeability transition pore (mPTP). *FEBS Open Bio*. 2019;9(9):1617–1622. doi:10.1002/2211-5463.12703
69. Li L, Sha Z, Wang Y, et al. Pre-treatment with a combination of Shenmai and Danshen injection protects cardiomyocytes against hypoxia/ reoxygenation- and H2O2-induced injury by inhibiting mitochondrial permeability transition pore opening. *Exp Ther Med*. 2019;17(6):4643–4652. doi:10.3892/etm.2019.7462
70. Chen S, Lv X, Hu B, et al. Critical contribution of RIPK1 mediated mitochondrial dysfunction and oxidative stress to compression-induced rat nucleus pulposus cells necroptosis and apoptosis. *Apoptosis*. 2018;23(5–6):299–313. doi:10.1007/s10495-018-1455-x
71. Semenov KN, Ageev SV, Kukaliia ON, et al. Application of carbon nanostructures in biomedicine: realities, difficulties, prospects. *Nanotoxicology*. 2024;18(2):181–213. doi:10.1080/17435390.2024.2327053
72. Xu C, Liu Q, Liu H, Zhang C, Shao W, Gu A. Toxicological assessment of multi-walled carbon nanotubes in vitro: potential mitochondria effects on male reproductive cells. *Oncotarget*. 2016;7(26):39270–39278. doi:10.18632/oncotarget.9689
73. Bernabò N, Fontana A, Sanchez MR, et al. Graphene oxide affects in vitro fertilization outcome by interacting with sperm membrane in an animal model. *Carbon*. 2018;129:428–437. doi:10.1016/j.carbon.2017.12.042
74. Tabandeh MR, Samie KA, Mobarakeh ES, Khadem MD, Jozaie S. Silver nanoparticles induce oxidative stress, apoptosis and impaired steroidogenesis in ovarian granulosa cells of cattle. *Animal Reprod Sci*. 2022;236:106908. doi:10.1016/j.anireprosci.2021.106908
75. Liou G-Y, Storz P. Reactive oxygen species in cancer. *Free Radical Res*. 2010;44(5):479–496. doi:10.3109/10715761003667554
76. Zhang Q, Ren J, Wang F, et al. Mitochondrial and glucose metabolic dysfunctions in granulosa cells induce impaired oocytes of polycystic ovary syndrome through Sirtuin 3. *Free Radic Biol Med*. 2022;187:1–16. doi:10.1016/j.freeradbiomed.2022.05.010
77. Mao J, Guo R, Yan L-T. Simulation and analysis of cellular internalization pathways and membrane perturbation for graphene nanosheets. *Biomaterials*. 2014;35(23):6069–6077. doi:10.1016/j.biomaterials.2014.03.087
78. Wang Q, Zhai X, Crowe M, et al. Heterogeneous oxidization of graphene nanosheets damages membrane. *Sci China*. 2019;62(6):064611. doi:10.1007/s11433-018-9317-7
79. Crowe M, Lai Y, Wang Y, et al. A proteoliposome method for assessing nanotoxicity on synaptic fusion and membrane integrity. *Small Methods*. 2017;1(11):1700207. doi:10.1002/smtd.201700207
80. Shao X, Fang Z, Li M, et al. Graphene oxide nanosheets induce mitochondrial fragmentation by cutting through membrane. *ACS Mater Lett*. 2023;5 (9):2308–2316. doi:10.1021/acsmaterialslett.3c00177
81. Xiao D, He H, Huang W, Oo TL, Wang A, He L-F. Analysis of mitochondrial markers of programmed cell death. *Plant Programmed Cell Death*. 2017;1743:65–71. doi:10.1007/978-1-4939-7668-3_6
82. Yang Q, Wang Y, Yang Q, et al. Cuprous oxide nanoparticles trigger ER stress-induced apoptosis by regulating copper trafficking and overcoming resistance to sunitinib therapy in renal cancer. *Biomaterials*. 2017;146:72–85. doi:10.1016/j.biomaterials.2017.09.008
83. Xiaoli F, Junrong W, Xuan L, et al. Prenatal exposure to nanosized zinc oxide in rats: neurotoxicity and postnatal impaired learning and memory ability. *Nanomedicine*. 2017;12(7):777–795. doi:10.2217/nnm-2016-0397
84. Guo C, Ma R, Liu X, et al. Silica nanoparticles induced endothelial apoptosis via endoplasmic reticulum stress-mitochondrial apoptotic signaling pathway. *Chemosphere*. 2018;210:183–192. doi:10.1016/j.chemosphere.2018.06.170
85. Holczer M, Hajdú B, Lőrincz T, Szarka A, Bánhegyi G, Kapuy O. A double negative feedback loop between mTORC1 and AMPK kinases guarantees precise autophagy induction upon cellular stress. *Int J Mol Sci*. 2019;20(22):5543. doi:10.3390/ijms20225543
86. Bhardwaj JK, Paliwal A, Saraf P, Sachdeva SN. Role of autophagy in follicular development and maintenance of primordial follicular pool in the ovary. *J Cell Physiol*. 2021;237(2):1157–1170. doi:10.1002/jcp.30613

International Journal of Nanomedicine

Dovepress
Taylor & Francis Group

Publish your work in this journal

The International Journal of Nanomedicine is an international, peer-reviewed journal focusing on the application of nanotechnology in diagnostics, therapeutics, and drug delivery systems throughout the biomedical field. This journal is indexed on PubMed Central, MedLine, CAS, SciSearch®, Current Contents®/Clinical Medicine, Journal Citation Reports/Science Edition, EMBase, Scopus and the Elsevier Bibliographic databases. The manuscript management system is completely online and includes a very quick and fair peer-review system, which is all easy to use. Visit http://www.dovepress.com/testimonials.php to read real quotes from published authors.

Submit your manuscript here: https://www.dovepress.com/international-journal-of-nanomedicine-journal